Carrier carrying capacity of one-step grown suspended carbon nanotube bridge with carbon nanotube contact electrodes: For practical one-dimensional electronics

Yun-Hi Lee,[a] Jong-Hee Lee, S. J. Chung, and S. Lee
National Research Laboratory, Department of Physics, Korea University, Anamdong, Seoul 136-713, Korea

B. K. Ju
Division of Electrical and Electronic Engineering, Korea University, Seoul 136-701, Korea

(Received 11 May 2006; accepted 26 June 2006; published online 16 August 2006)

The authors report the carrier transport and electrical breakdown behaviors of micron-long-channel suspended carbon nanotube (CNT) of carbon-based one-dimensional junction with CNTs as drain and source electrodes. The structure consisted of bundle-type CNT electrode–a CNT channel–bundle-type CNT electrode, produced by one-step *in situ* direct growth via a unique diluted magnetic nanothick film catalyst at low temperature. The unique suspended all-one-dimensional CNT-based junction provides some insights into recent reports that an electrical breakdown of CNTs can be induced not by the contact problem but by the nonhomogeneously Joule heating along nanotube without release of heat into contacts by the observed breakdown at midlength of a $1-2$ μm long channel. The high current carrying all-CNT junction with bridging yield of 90% and stable operation at fixed voltage level can contribute into realization of practical integrated nanoelectronics such as interconnector and transistor via junction formation of one-step final process. © *2006 American Institute of Physics*. [DOI: 10.1063/1.2336084]

One reason for the focused research is the excellent electrical properties of the CNTs such as ballistic electric conduction and ballistic phonon conduction, which the relation between heat dissipation and electrical conduction is of importance because of their potential use in probing the intrinsic properties of one-dimensional nanotubes as well as practical applications of active components and/or interconnectors for nanoelectronics and nanomechanics.[1–12] When the length of a CNT is shorter than the electron mean free path (mfp), the carrier transport is ballistic, in which event, each conduction channel contributes to the total conductance a quantum conductance (G_0). According to the recent results of Cao *et al.* who heated MWNTs with an electrical current and monitored the temperature, CNTs on substrate show the relation P (electrical breakdown power for each shell in MWNTs) $\sim L$ (length of channel) while freestanding tubes approximately follow $P \sim 1/L$ behavior.[13] On the other hand, self-consistent quantum simulations by Guo *et al.*[14] suggest that using an array of parallel CNTs as the transistor one-dimensional (1D) channel and/or 1D contact as source and drain electrodes would significantly reduce the parasitic capacitance per tube and, thereby, improve frequency performance in ac applications.

In this study, we report the high yield fabrication of *in situ* suspended all-1D nanotube-based junction with virtual source and drain electrodes made of 1D CNTs onto SiO_2-Si-back gate substrate and discuss their characteristic transport behaviors including the mentioned points of contact resistance as well as electrical breakdown. Technically, we made all-CNT-based suspended junctions by *in situ* lateral growth based on our approaches.[15] First, we used the one-step process method to grow suspended CNTs between photolithographically defined patterned electrodes. Second, in order to realize all-CNT based 1D three terminal junction by the one-step process, we adopted specially designed diluted magnetic metal doped thin films [i.e., diluted magnetic semiconductor (DMS)] as a catalyst for the growth of both a single lateral CNT channel and bundle-type CNT electrodes.[16] Our rapid thermal chemical vapor deposition (CVD) process and one-step growth resulted easily in one to two multiple or single suspended CNT bridges between *in situ* formed CNT electrodes, which were less than about 10 nm in diameter. During the electrical study, the as-formed CNTs were used as drain and source electrodes without any additional treatments.

The suspended $1-3.5$ μm long CNTs with two to five walls selected at random after few tens of batch processes show a well-crossing bridge, while the CNT electrodes consisted of an entangled network grown only on prepatterned DMS catalysts, as clearly seen in Fig. 1. Figure 2(a) shows the corresponding drain current (I_{sd}) versus drain-source voltage characteristics of randomly selected all-CNT-based junction. The linear relationship between the I_{sd} and V_{sd} at a low drain-source bias indicated the formation of a fairly good Ohmic contact *between* the entangled CNT electrodes and the individual CNT bridge. In the higher voltage regime,

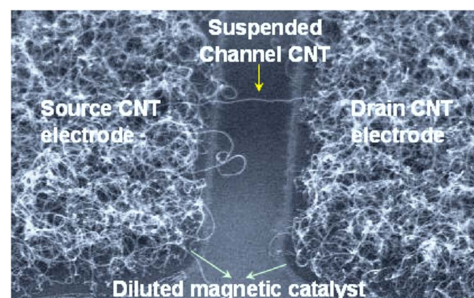

FIG. 1. (Color online) SEM image of a typical CNT junction with 1D-CNT contact electrodes fabricated in this work. The scale bar represents 1 μm.

[a]Author to whom correspondence should be addressed; electronic mail: yh-lee@korea.ac.kr

 © 2006 American Institute of Physics
Downloaded 14 Feb 2007 to 163.152.27.28. Redistribution subject to AIP license or copyright, see http://apl.aip.org/apl/copyright.jsp

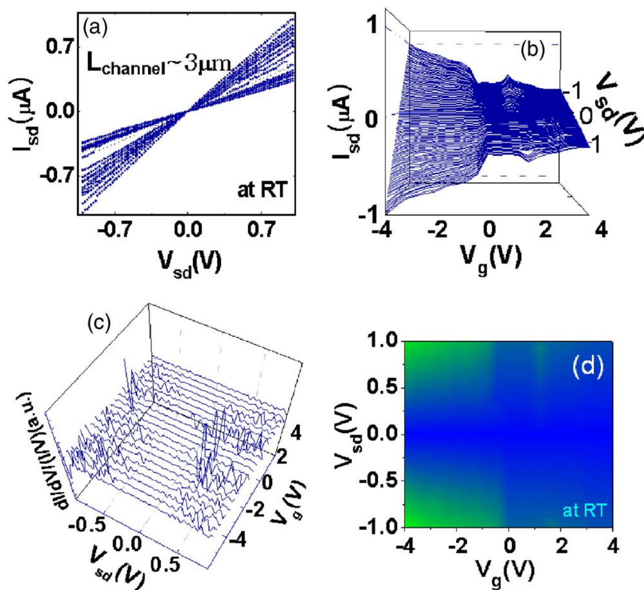

FIG. 2. (Color online) (a) I_{sd} vs V_{sd} characteristics as a function of gate voltage(V_g). (b) Measured I_{sd} vs V_g characteristics for CNTs with length of 2 μm. (c) $[dI/dv]/(I/V)$ vs V characteristics as a function of V_g. (d) I_{sd}-V_{sd}-V_g plot showing the nonexistence of Coulomb blockade.

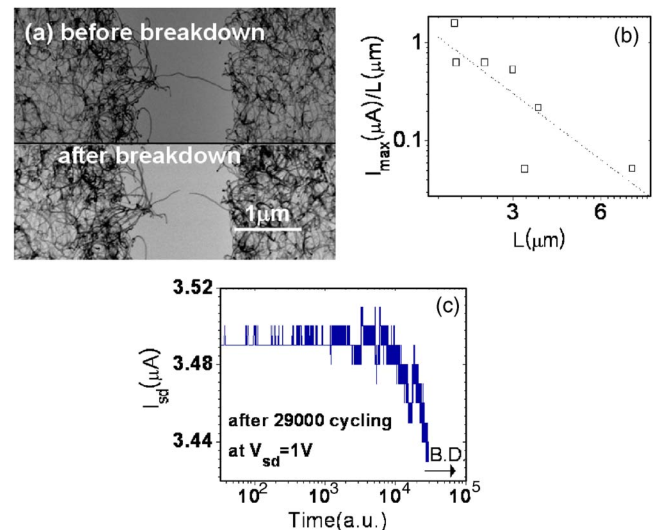

FIG. 3. (Color online) (a) SEM images showing before and after catastrophic electrical breakdown of the CNT junction with virtual CNT contact electrodes. One can clearly see the breaking of the middle section of the CNT channel not contact portion. (b) Channel current vs channel length ($L_{channel}$). (c) Channel current (I_{sd}) with cycling time under constant electric field stressing for the short channel.

channel current starts to increase drastically and then drops suddenly to a lower level, indicating some failure breakdown or peeling shells. The successive event repeated until breakdown without current saturation.[18] The nonsaturated current behavior, i.e., an evidence of ballistic transport, before breakdown differed from the observation by other groups who used normal metal (Pt, Au, etc.)-CNT contacts with suspended CNT bridge. A very recent report by Huan group addressed the nonsaturated current of MWNTs, though they used an individual MWNT with Au electrodes, in which every wall of the MWNTs is contacted by the electrodes, and scanning tunneling microscopy probe was contacted on channel. They observed both the rapid increase of current and subsequent breakdown without current saturation. Here it is noticeable that our all-CNT junction showed similar behavior with the well end-contacted MWNTs of Huang *et al.*[7] and Javey *et al.*,[17] thus indicating real end-contacted CNT junctions.

Figure 2(b) shows gate voltage (V_g) reponse characteristics, which showed more *p*-type dominant behavior, accompanying still weak *n*-type conduction behavior. This response provides an evidence for Schottky barriers which affects the performance of CNT-FETs (field effect transistors) in most other geometries with normal bulk metal electrodes is still present in this junction of 1D electrode–1D channel–1D electrode. The existence of two barriers for electrons and holes, respectively, of approximately equal height was confrimed through our previous result.[18] The subthreshold behavior of our CNT-FET with 1 μm thick gate oxide, i.e., S, subthreshold swing is very high S values of approximately 3 V/decade. Such high values of S are not consistent with bulk switching mechanism which give 65 mV/decade in the long channel single-walled nanotube (SWNT) limit theoretically.

Considering the fact that the broad range of contact properties in metal-contacted CNT junctions was reported by others, reproducible figure of merit in the junction is one of the merit in the application of both nanointerconnector and switching components.

Figures 2(c) and 2(d) show a two-dimensional gray scale plot of $[dI/dV]/(I/V)$ as a function of bias (V_{sd}) and gate voltages (V_g) for an all-CNT junction at room temperature. The $dI/dV/(I/V)$ corresponds to density of states of an individual CNT bridge formed in this junction and more suppressed around the zero V_g bias, the size of the voltage gaps is widened in the positive V_g regime without the bias voltage of V_{sd}, and the dark regions can be identified, in which the conductance is more suppressed. Two additional bright regions appearing at positive V_g regimes; these regions indicate the possibility of ambipolar operation in our all-1D junction.

Figure 3(a) shows the typical breakdown scanning electron microscopy (SEM) images of a series of devices after measurements at room temperature under ambient atmosphere and their corresponding *I*-*V* characteristics just before and after catastrophic failure. One can see that the middle position of the suspended CNT bridge was burned and breakdown finished in the middle section of the nanotube, and not at the contacts. Considering the fact that our junction consisted of all-one-dimensional channel of same material characteristics, i.e., good end-contacted junction, the breakdowns in the center of the channel indicate somewhat differences between CNTs as electrodes and the channel CNT in electrical and thermal characteristics. Furthermore, unhomogeneous Joule heating along the channel assumed the previous report is likely to operate during the carrier transport and their breakdown. According to the very recent theoretical analysis by Kuroda *et al.*[9] the temperature difference (ΔT) in the middle of the CNT as a function of I_{sd} for different CNT lengths (ℓ) generated power along CNTs is given by $q^*=JF$, where $j=I/A$ is current density through the effective cross section A and the electric field F is given by $F=|V_{ds}/L|$. Then, the temperature profile along CNT is given by $\Delta T(x)=q/\gamma LS[1-\cosh(\Gamma x)/\cosh(\Gamma L/2)]$ where $\Gamma=\sqrt{\gamma/\kappa}$, K is thermal conductivity, and $\gamma(=\kappa_{sub}/td)$ is the coupling coefficient with the substrate. The temperature between the middle of the CNT channel and electrodes can take place depending on the value of ΓL. If one uses the standard

Downloaded 14 Feb 2007 to 163.152.27.28. Redistribution subject to AIP license or copyright, see http://apl.aip.org/apl/copyright.jsp

value for $\kappa(30\ \mathrm{W/cm\,K})$ and $\gamma(10^{11}\ \mathrm{W\,cm^{-3}\,K^{-1}})$ for our junction, the rise up to the typical catastrophic breakdown temperature of 900 K (Ref. 12) is instantly reached even the channel current is about far below microampere level. In our case, the coupling parameter value to the Si substrate is extremely lower as compared to the case of other junctions of micron-sized normal metal CNT by others, thus the temperature profile along channel follows parabolic shape with maximum value at the middle of the channel. Furthermore, dissipation occurs over longer length while heat release mainly takes place largely through the ambient air, which is in contrast with the conventional junction with a large substrate and/or micron-sized normal contact metals. Another interesting point is that both CNT electrodes act as additional active channel for carriers. This viewpoint suggests that few tens of micrometer length CNTs consisting of electrodes are involved in the conduction itself like virtual channel. If we combine the obtained fact that slight lower current than normal metal junction with very long carrier path including electrode portion, participating as virtual paths, path for the conduction is very longer than geometrical expectation of spacing between electrode CNT (i.e., drain) and electrode CNT (source). Therefore, we can conclude that the observed current reaching a few microamperes is significant level in all-CNT-based junction, providing promising future for the nanoelectronics. As a result, the longer the nanotube channel as fabricated in this, the faster the rise in temperature as the current increases over the critical level. Also, it should be considered that if the CNT electrodes are in good contact with the CNT channel and, thus, good thermal conductivity is maintained, heat generated by resistive heating would not accumulate at the contacts.

Based on the electron-phonon scattering as most dominant sources of the resistive heating of CNTs, short mfp for optical phonon scattering suggests that truly ballistic transport in CNTs under critical bias requires length scaling on the nanometer scale. The shortest metallic SWNT that Dai and co-workers fabricated was ~ 10 nm long between Pd electrodes. Up to 70 μA current can flow through the 10 nm tube at $V_{ds} \sim 2.6$ V, beyond which the nanotube breaks down. To examine the length dependence, we measured the channel current as a function of channel length. Figure 3(b) shows log-log plots of I_{sd} vs L. Our suspended all-CNT junction approximately follows the relation of $I_{sd}(\mu\mathrm{A})/L(\mu\mathrm{m}) \sim L^{-2.2}$, suggesting nonballistic transport. Therefore, significant scattering occurs along the length of the CNTs. To clearly determine the transport type of this junction, whether ballistic or diffusive, mean free path is estimated based on the Einstein relation of electrical conductance $G = (\pi dm/L)e^2 D\nu$, where the symbols have conventional meaning. We estimated the mfp which is given by $1/\lambda_{mfp} = \pi dm\rho G_0(k_B T/\hbar\nu_F)$ with $d = 10-20$ nm, m (number of walls) $= 5-10$ depending on batch to batch, $R = 20\ \mathrm{k\Omega} - 2\ \mathrm{M\Omega}$, and $L = 1.2-100\ \mu$m. We obtain a minimum average $\lambda_{mfp} = 4$ nm, depending on the diameter and length of CNT. The value is lower than 10 nm, which was estimated by both Huang *et al.*[7] and Javey *et al.*[17] However, considering their estimated value of $\lambda_{mfp} = 10$ nm was obtained for 200 nm spacing CNT channel, it is sure that micrometer-length channels in this work showed well functioning. Note that an exact value of CNT channel cannot be inserted into the equation because it can be expected that the entangled electrode CNTs would easily participate in the conduction like a virtual channel due to 1D characteristics. Recently, a series of experiment and theory has shown that thermal conduction in suspended CNT differs from that of supported nanotubes. For supported (i.e., lying on a substrate) CNTs, the substrate-nanotube interaction could provide the cooling pathway via heat conduction into substrate (a large reservoir) and also, mechanically flatten the channel. Meanwhile suspended CNTs, not only the suspended part but also the electrodes, have only thermal source without efficient thermal sink except ambient air.

Finally, we examined the time-dependent channel current as a function of operating time, as shown in Fig. 3(c). In spite of the fluctuations, several observations can be made, illustrated by the characteristics in the figure. The minimum and maximum currents in the device did not change by more than 5% within measured time duration. The observation that these devices are stable indicates that the CNT contacts can be adopted as an electrode carrying high current as well as good interconnector for nanoelectronics which were formed via direct one-step method by the diluted magnetic catalyst. Further experiments are necessary to examine the exact origin of the catastrophic breakdown and enhance current capacity in suspended 1D channel with 1D-CNT contacts for practical all-CNT-based circuit. Also, the experimental examination of our junction will be required on theoretical contact dependence of carrier injection in terms of a weak hybridization with a large contact length between the cantact metal and the nanotube channel.[19]

This work was supported by PBRG of KRF, Nano Core Technology Project (KOSEF) and by the National Research Laboratory Program of KOSEF in Korea.

[1] W. Honlein, Jpn. J. Appl. Phys., Part 1 **41**, 4370 (2002).
[2] Z. Chen, J. Appenzeller, Y. M. Lin, J. S. Oakley, A. G. Rinzler, J. Tang, S. J. Wind, P. M. Solomon, and P. Avouris, Science **311**, 1735 (2006).
[3] M. Bockrath, D. H. Codden, P. L. McEuen, N. G. Chopra, A. Zettl, A. Thess, and R. E. Smally, Science **275**, 1922 (1997).
[4] S. J. Tans, A. R. M. Verschueren, and C. Dekker, Nature (London) **393**, 49 (1998).
[5] Z. Chen, J. Appenzeller, Y. M. Liu, J. S. Oakley, A. G. Rinzler, J. Tang, S. J. Wind, P. M. Solomon, and P. Avouris, Science **211**, 1735 (2006).
[6] Vera Sazonova, Yuval Yaish, Hande Üstünel, David Roundy, Tomás A. Arias, and Paul L. McEuen, Nature (London) **431**, 284 (2004).
[7] J. Y. Huang, S. Chen, S. H. Jo, Z. Wang, D. X. Han, G. Chen, M. S. Dresselhaus, and Z. F. Ren, Phys. Rev. Lett. **94**, 236802 (2005).
[8] S. Sapmaz, P. J. Herrero, Y. M. Blanter, C. Dekker, and H. S. J. van der Zant, Phys. Rev. Lett. **96**, 026801 (2006).
[9] M. A. Kuroda, A. Cangellaris, and J. P. Leburton, Phys. Rev. Lett. **95**, 266803 (2005).
[10] B. Bourlon, D. C. Glattli, B. Placais, J. M. Berroir, C. Miko, L. Forro, and A. Bachtold, Phys. Rev. Lett. **92**, 026804 (2004).
[11] H. J. Li, W. G. Lu, J. J. Li, X. D. Bai, and C. Z. Gu, Phys. Rev. Lett. **95**, 086601 (2005).
[12] H.-Y. Chiu, V. V. Deshpande, H. W. Ch. Postma, C. N. Lau, C. Miko, L. Forro, and M. Bockrath, Phys. Rev. Lett. **95**, 226101 (2005).
[13] J. Cao, Q. Wang, and H. J. Dai, Nat. Mater. **4**, 745 (2005).
[14] J. Guo, S. Hasan, A. Javey, G. Bosman, and M. Lundstrom, IEEE Trans. Nanotechnol. **4**, 715 (2005).
[15] Y.-H. Lee, Y. T. Jang, C. H. Choi, D. H. Kim, C. W. Lee, J. E. Lee, Y. S. Han, S. S. Yoon, J. K. Shin, S. T. Kim, E. K. Kim, and B. K. Ju, Adv. Mater. (Weinheim, Ger.) **13**, 1371 (2001).
[16] Y.-H. Lee, J. M. Yoo, J. A. Lee, S. Y. Ahn, J. Joo, S. Lee, D. H. Kim, K. J. Song, and B. K. Ju, Appl. Phys. Lett. **87**, 121915 (2005).
[17] A. Javey, J. Guo, Q. Wang, M. Lundstrom, and H. J. Dai, Nature (London) **424**, 654 (2003).
[18] Y.-H. Lee, J. M. Yoo, J. H. Lee, and B. K. Ju (submitted).
[19] N. Nemec, D. Tomanek, and G. Cuniberti, Phys. Rev. Lett. **96**, 076802 (2006).

Downloaded 14 Feb 2007 to 163.152.27.28. Redistribution subject to AIP license or copyright, see http://apl.aip.org/apl/copyright.jsp